
INVESTIGATION ON CENTRALITY MEASURES AND OPINION DYNAMICS IN TWO-LAYER NETWORKS WITH REPLICA NODES

A PREPRINT

 **Chi Zhao**

Saint Petersburg State University,
7/9 Universitetskaya nab.,
Saint Petersburg, 199034, Russia
st081292@student.spbu.ru

 **Elena Parilina**

Saint Petersburg State University,
7/9 Universitetskaya nab.,
Saint Petersburg, 199034, Russia
School of Mathematics and Statistics,
Qingdao University,
Qingdao, 266071, PR China
e.parilina@spbu.ru

September 19, 2024

ABSTRACT

We examine two-layer networks and centrality measures defined on them. We propose two fast and accurate algorithms to approximate the game-theoretic centrality measures and examine connection between centrality measures and characteristics of opinion dynamic processes on such networks. As an example, we consider a Zachary's karate club social network and extend it by adding the second (internal) layer of communication. Internal layer represents the idea that individuals can share their real opinions with their close friends. The structures of the external and internal layers may be different. As characteristics of opinion dynamic processes we mean consensus time and winning rate of a particular opinion. We find significantly strong positive correlation between internal graph density and consensus time, and significantly strong negative correlation between centrality of authoritative nodes and consensus time.

Keywords Opinion dynamics · Centrality measure · General concealed voter model · Zachary's karate club

1 Introduction

The models of opinion dynamics can be divided into macroscopic and microscopic. Macroscopic models including Ising model [1], Sznajd model [2], voter model [3], concealed voter model (CVM) [4, 5], and macroscopic version of general concealed voter model (GCVM) [6] examine social networks using statistical-physical and probability-theoretical methods to analyze distribution of opinions over time.

Within GCVM [6], it is supposed that the individuals communicate in two layers (internal and external) and can interact in internal or private layer, which makes this model different from CVM, where individuals do not express their true opinions in the internal layer.

Well-known examples of microscopic models of opinion dynamics are DeGroot model [7], Friedkin-Johnsen (F-J) model [8], and bounded confidence models [9, 10]. In the F-J model, actors can also factor their initial prejudices into every iteration of opinion [11]. The models of opinion dynamics based on DeGroot and F-J models, and Markov chains with possibility to control agents' opinions are proposed in [12, 13, 14, 15]. The levels of influence and opinion dynamics with the presence of agents with different levels of influence are examined in [16, 17].

A bounded confidence model (BCM) describes the opinion dynamics, in which agents ignore opinions that are very far from their own opinions [18, 19]. The BCM includes two essential models: the Deffuant-Weisbuch model (D-W) proposed in paper [9], and the Hegselman-Krause (H-K) model introduced in the work [10]. In the D-W model, two individuals are randomly chosen, and they determine whether to interact according to the bounded confidence [20].

The micro version of GCVM is introduced in [21, 22], and the difference between macro and micro versions is the following. In the micro version, we do not need to adjust the simulation program according to different network structures, as long as network structure is given, the program automatically produces simulations. Therefore, we can use this program to simulate real networks. But for the macro version, we should adjust the corresponding state transition formulae for different network structures.

Since network structure in GCVM is two-layer, it is interesting to examine how not only this two-layer structure in general, but also network characteristics, e.g. different centrality measures [23], affect opinion dynamics and resulting opinion in consensus if it is reached. In this work, we consider two key performance indicators of opinion dynamics, namely, winning rate and consensus time and their relationship with network characteristics.

We focus on centrality measures, considering them as important network characteristics reflecting individual’s social power (influence centrality). Centrality measures can be used to identify the most powerful nodes in the network, and information about them is crucial for opinion spreading. The most common centrality measures proposed for one-layer networks are betweenness centrality [24], closeness centrality [25, 26, 27], and degree centrality [28]. Some centrality measures are based on random walk, such as random walk occupation centrality [29] which is the frequency of a node in the network being accessed during a random walk; random walk betweenness centrality [30], that is the proportion of the paths through a node to all paths during a random walk. The latter measure does not depend on the shortest path, so it can be considered as a more general one than betweenness centrality. Random walk closeness centrality is a variant of closeness centrality [29], the computation of which is based on the mean first-passage time (MFPT). The analytical expressions of random-walk based centrality measures can be found in [29].

In this paper, we also consider game-theoretic network centralities borrowed from cooperative game theory. A good review on game-theoretic network centrality measures is written by Tarkowski [31]. The Shapley value [32] and the Myerson value [33] are the cooperative solutions which are proposed as allocations of the total payoff among players based on their marginal contributions. In the paper [34], the authors introduce how to use Shapley value to determine the top- k nodes in the social network. Mazalov et al. in [35] proposed a game-theoretic centrality measure for the weighted graph based on the Myerson value. Mazalov and Khitraya introduced a modified Myerson value for unweighted undirected graphs calculated for a special characteristic function considering not only simple paths but also cycles [36]. In the next work of these authors [37], the concept of integral centrality for unweighted directed graph is introduced, and a rigorous mathematical proof that this centrality measure satisfies the Boldi-Vigna axioms [38] is provided.

In this paper, first we extended our previous work [39] by considering additional centrality measures and examining the relationship between centrality measures and opinion dynamics in GCVM. Second, we proposed two fast and accurate algorithms to approximate the game-theoretic centrality measures and tested them on randomly generated networks and Zachary’s karate club network. The preliminary conclusion made from this research is that there is a significantly strong positive correlation between internal graph density and consensus time, and significantly strong negative correlation between centrality of “authoritative” or most central nodes and consensus time. The proposed algorithms efficiently approximate the Shapley and Myerson values in randomly generated networks with high accuracy. Additionally, our algorithms successfully determine the two most influential nodes in the Zachary’s karate club network.

The rest of this paper is organized as follows. Section 2 introduces multi-layer network with replica nodes. Network properties and particular centrality measures are discussed in Section 3, where we also introduce algorithms to approximate the Shapley and Myerson values. Section 4 describes simulation experiments and results of these experiments. We briefly conclude and discuss our future work in Section 5.

2 Multi-layer networks with replica nodes

2.1 Multi-layer network

A multilayer network is a network formed by several networks that evolve and interact with each other [40].

2.2 Replica nodes

In a multilayer network with replica nodes there is a one-to-one mapping of the nodes in different layers and corresponding nodes are called replica nodes. Since there is a one-to-one mapping between the nodes in different layers, every layer is formed by the same number of nodes [40].

2.3 Two-layer networks with replica nodes

We use the following notations to define a two-layer (external and internal layers) network with replica nodes:

- N : number of nodes in each layer;
- $a_i = (a_i^E, a_i^I)$: one-to-one mapping of node i in the external and internal layer, where a_i^E (a_i^I) is a representation of node i in the external (internal) layer;
- $G_E(\mathcal{V}_E, \mathcal{E}_E)$: predefined external network, where $\mathcal{V}_E = \{a_i^E\}$ and \mathcal{E}_E represent a set of individuals and set of edges in the external layer, respectively;
- $G_I(\mathcal{V}_I, \mathcal{E}_I)$: predefined internal network, where $\mathcal{V}_I = \{a_i^I\}$ and \mathcal{E}_I represent a set of individuals and set of edges in the internal layer, respectively;
- $\mathcal{E}_C = \{(a_i^E, a_i^I) | i = 1, \dots, N\}$: edges connecting replica nodes.

A two-layer network with N individuals/agents can be defined as¹:

$$G(\mathcal{V}, \mathcal{E}), \quad (1)$$

where $\mathcal{V} = \mathcal{V}_E \cup \mathcal{V}_I$, $|\mathcal{V}_E| = |\mathcal{V}_I| = N$, and $\mathcal{E} = \mathcal{E}_E \cup \mathcal{E}_I \cup \mathcal{E}_C$.

2.4 Two-layer network simplification

Two-layer network $G(\mathcal{V}, \mathcal{E})$ is composed of external network $G_E(\mathcal{V}_E, \mathcal{E}_E)$, internal network $G_I(\mathcal{V}_I, \mathcal{E}_I)$ with the set of edges \mathcal{E}_C connecting nodes between layers. Two-layer networks can also be represented by an adjacency matrix. The adjacency matrix of a two-layer network is a block matrix, where the diagonal blocks are the adjacency matrices of the external and internal layers, and the off-diagonal blocks are the adjacency matrices of the connections between external and internal layers.

The adjacency matrix of $G(\mathcal{V}, \mathcal{E})$ is as follows:

$$A = \begin{bmatrix} A_{EE} & A_{EI} \\ A_{IE} & A_{II} \end{bmatrix} \quad (2)$$

where A_{EE} is the adjacency matrix of the external layer, A_{EI} is the adjacency matrix of the connections between external and internal layers, A_{IE} is the adjacency matrix of the connections between internal and external layers, and A_{II} is the adjacency matrix of the internal layer. For undirected graphs in both layers, the adjacency matrix A is symmetric.

Keeping in mind an binary opinion dynamics model presented in [6], we define the rates of coping opinions from one node to another:

- π_{c_e} : external copy rate with which an individual is copying opinion of his/her external neighbor if they both are randomly chosen;
- π_{c_i} : internal copy rate with which an individual is copying opinion of his/her internal neighbor;
- π_e : externalization rate with which an individual is behaving as a hypocrisy² choosing to publicly express his/her internal opinion;
- π_i : internalization rate with which an individual being hypocrisy accepts his/her external opinion.

We propose a way how to transform a two-layer network $G(\mathcal{V}, \mathcal{E})$ with the given parameters $\pi_{c_e}, \pi_{c_i}, \pi_e, \pi_i$ of opinion dynamics to a one-layer weighted network. We can define a matrix of weights as follows:

$$W' = \pi_{c_e} \cdot A_{EE} + \pi_{c_i} \cdot A_{II} + \pi_i \cdot \Lambda_E + \pi_e \cdot \Lambda_I, \quad (3)$$

where Λ_E and Λ_I are $N \times N$ diagonal matrices, and the elements on the diagonal represent the degrees of nodes in external and internal layers, respectively. Furthermore, we use $w'_{i,j}$ to represent the elements of matrix W' and define a new weighted network $G'(\mathcal{V}', \mathcal{E}', W')$, where $\mathcal{V}' = \{1, 2, \dots, N\}$ is the set of nodes, $\mathcal{E}' = \{(i, j) | w'_{i,j} \neq 0, i, j \in \mathcal{V}'\}$ is the set of edges, and W' is the matrix of weights.

Based on a new weighted network $G'(\mathcal{V}', \mathcal{E}', W')$, we proposed two game-theoretic centrality measures which will be discussed in Section 3.3.

¹Opinion dynamic models in two-layer networks with replica nodes was introduced in [22] and further discussed in [21] and [39].

²By hypocrisy we mean a node having different opinions in external and internal layers.

2.5 Zachary’s karate club in a two-layer network setting

As an example of a social network, we consider Zachary’s karate club network representing friendship relations among 34 members of a karate club at the US university in the 1970s [41]. The study became famous in data and network analytical literature since it highlighted a conflict between manager (Node 0) and director (Node 33), which eventually led to the split of the club into two groups. One-layer Zachary’s karate club network is represented in Fig. 1. The blue and red colors of nodes represent two opinions in the social network.

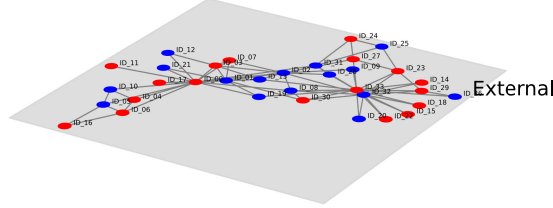


Figure 1: One-layer Zachary’s karate club network

Fig. 2 shows how one-layer Zachary’s Karate Club network can be extended into a two-layer network if we add an internal layer of communication between agents. If we consider binary opinion dynamics models, in the concealed voter model (CVM) [4, 5], the nodes in the internal layer are not connected, i.e. internal layer is represented by an empty graph (see Fig. 2a), while in the general concealed voter model (GCVM) [21, 22, 6] there may be nonempty network representing internal communication of agents. In Fig. 2b we represent a star internal structure. The colors in Fig 2 represent individuals’ opinions.

The color, blue or red, is randomly initialized for the given parameters, these are (i) probability of having red initial opinion for the basic voter model on one-layer network, (ii) probabilities of having red initial opinion in external, internal, and in both layers for CVM and GCVM models.

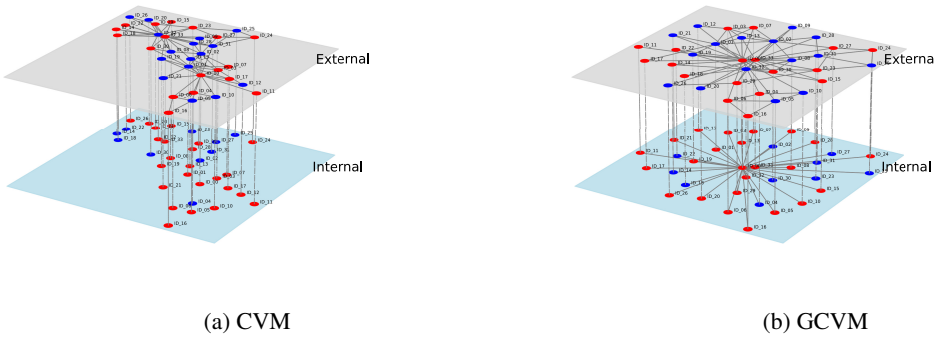


Figure 2: Two-layer networks used in CVM and GCVM: (a) CVM: two-layer network with external Zachary’s karate club and empty internal layer, (b) GCVM: two-layer network with external Zachary’s karate club and star internal layer.

In the basic voter model (BVM, see [3]), there is only one layer, as shown in Fig. 1, and each individual holds one of two opinions (red or blue). At each step, a random individual selects a random neighbor and adopts his/her neighbor’s opinion with the copying rate π_{c_e} . This process repeats until everyone in the network holds the same opinion, i.e. reaching a consensus. The opinion dynamics process in CVM [4, 5] and GCVM [21, 22, 6, 39] is implemented on a two-layer network (see Fig. 2a and 2b). In the CVM, individuals in the internal layer do not communicate, while in GCVM, individuals in the internal layer can communicate. The opinion dynamics process in CVM and GCVM is similar to BVM, but have more options: in the CVM, individuals can his/her internal opinion publicly with externalization rate π_e or accept his/her external opinion with internalization rate π_i . These two options do not exist in the BVM, while in GCVM, individuals can copy their internal neighbors’ opinion with internal copy rate π_{c_i} , which is not allowed in the CVM.

3 Centrality measures in one- and two-layer networks

In this section, we represent several centrality measures. Some of them are defined for one-layer networks and can be applied for two layers separately, some of them take into account the multi-layer structure of a network. We also introduce game-theoretical centrality measures and provide an algorithm to calculate their approximation when the network contains large number of nodes.

Definition 1 A pairwise average shortest path for an external layer d_E in a two-layer network is

$$d_E = \sum_{s,t \in \mathcal{V}_E} \frac{d_E(s,t)}{n_E(n_E - 1)}, \quad (4)$$

where $d_E(s,t)$ is a length of the shortest path between nodes s and t in the external layer, \mathcal{V}_E is a set of nodes in the external layer, $n = |\mathcal{V}_E|$ is a number of nodes in the external layer. Similarly, we can define pairwise average shortest path for an internal layer denoted by d_I .

Definition 2 A graph density is a ratio of the number of edges $|\mathcal{E}|$ with respect to the maximal number of edges. Since internal layer is represented by an undirected graph, we define an internal graph density as in [42]:

$$D_I = \frac{2|\mathcal{E}_I|}{|\mathcal{V}_I|(|\mathcal{V}_I| - 1)}. \quad (5)$$

3.1 Classical centrality measures

In this section we briefly introduce some (most well-known) centrality measures defined for one-layer networks. In the rest of the paper, we use V to denote the set of nodes in a one-layer network.

3.1.1 Betweenness centrality

Betweenness centrality of a node introduced in [24] gives the number of geodesics between all nodes that contain this node. It reflects the level of node participation in the dissemination of information between other nodes in a graph. It is calculated by the formula:

$$C_b(v) = \frac{1}{n_b} \sum_{s,t \in V} \frac{\sigma_{s,t}(v)}{\sigma_{s,t}}, \quad (6)$$

where $\sigma_{s,t}$ indicates the number of shortest paths between nodes s and t , and $\sigma_{s,t}(v)$ is the number of shortest paths between nodes s and t containing node v . Normalization coefficient is $n_b = (|V| - 1)(|V| - 2)$ for $v \notin \{s, t\}$, otherwise $n_b = |V|(|V| - 1)$, where $|V|$ is the number of nodes in a one-layer network [23]. If $s = t$, $\sigma_{s,t} = 1$ and if $v \in \{s, t\}$, then $\sigma_{s,t}(v) = 0$.

3.1.2 Group betweenness centrality

Group betweenness centrality measure indicates a proportion of shortest paths connecting pairs of nongroup members that pass through the group (see [43]), and it is defined by formula:

$$C_{gb}(X) = \frac{1}{n_{gb}} \sum_{s,t \in V \setminus X} \frac{\sigma_{s,t}(X)}{\sigma_{s,t}}, \quad (7)$$

where $\sigma_{s,t}(X)$ is the number of shortest paths between nodes s and t passing through some nodes in group X . Normalization coefficient is $n_{gb} = (|V| - |X|)(|V| - |X| - 1)$, where $|X|$ is the number of nodes in group X .

3.1.3 Closeness centrality

In a connected graph, closeness centrality of node u is the reciprocal of a sum of lengths of the shortest paths between u and all other nodes in the graph [25, 26, 27]. When calculating closeness centrality, its normalized form is usually referred to as the one representing the average length of the shortest path instead of their sum, and it is calculated like this:

$$C_c(u) = \frac{n_c}{\sum_{v \in V \setminus \{u\}} d(v, u)}, \quad (8)$$

where normalization coefficient is $n_c = |V| - 1$.

3.1.4 Group closeness centrality

Group closeness centrality is the reciprocal of the sum of the shortest distances from the group to all nodes outside the group [43, 44, 45]. It is calculated as follows:

$$C_{gc}(X) = \frac{n_{gc}}{\sum_{v \in V \setminus X} d(v, X)}, \quad (9)$$

where $d(v, X)$ is the shortest distance between group X and v . Normalization coefficient is $n_{gc} = |V - X|$.

3.1.5 Degree centrality

Degree centrality of node v [28] is defined as

$$C_d(v) = \frac{v_d}{n_d}, \quad (10)$$

where v_d is a degree of node v , and normalization coefficient is $n_d = |V| - 1$.

3.1.6 Group degree centrality

Group degree centrality is the number of nodes outside the group connected with the nodes from this group [43, 44]. Normalized group degree centrality for group X is given by the formula:

$$C_{gd}(X) = \frac{|\{v_i \in V \setminus X | v_i \text{ is connected to } v_j \in X\}|}{n_{gd}}, \quad (11)$$

where normalization coefficient is $n_{gd} = |V| - |X|$.

3.2 Random walk based centralities

The second group of centrality measures is based on random walks, simple dynamical process that can occur on a network. Random walks can be also used to approximate other types of diffusion processes [46, 47, 29].

3.2.1 Random walk occupation centrality

The random walk occupation centrality [29] of node v is the probability of that node v being visited by a random walker during an infinitely long walk, and it is defined as

$$C_{rwoc}(v) = \lim_{t \rightarrow \infty} \frac{n_v(t)}{t}, \quad (12)$$

where $n_v(t)$ is the number of times node v is visited by a random walker during time interval t . Different exploration strategies can be used to calculate the occupation centrality, we use the uniform exploration strategy in this paper (i.e. each node jumps to its neighbor with the equal probability). In the weighted networks, jumping probabilities are proportional to the weights of the edges.

The analytical expressions of random walk occupation centrality with a uniform exploration strategy in interconnected multilayer networks are presented in [29].

3.2.2 Random walk betweenness centrality

The most common betweenness is the shortest path betweenness [24, 29], where the centrality of a node v is relative to the number of shortest paths between all pairs of nodes passing through v . However, in real networks, entities (rumors, messages, or internet packets) that travel the network do not always follow the shortest path [48, 29, 49]. Therefore, the random walk betweenness centrality of node v is defined as the number of random walks between any pair (s, d) of nodes that pass through node v [30]:

$$C_{rwbc}(v) = \frac{1}{n_{rwbc}} \sum_{\substack{s, t \in V \\ s \neq t \\ v \neq s, v \neq t}} \mathbf{1}_{v \in \text{Path}_{s \rightarrow t}}, \quad (13)$$

where $n_{rwbc} = 2N(N - 1)$ is the normalization coefficient. The indicator function $\mathbf{1}_{v \in \text{Path}_{s \rightarrow t}}$ is equal to 1 if node v is in the path between nodes s and t , and 0 otherwise. The $\text{Path}_{s \rightarrow t}$ is the random path between nodes s and t in the

network. Repeating the random walk process few times to get different random paths we get the average random walk betweenness centrality.

It will be useful to get the analytical expression of random walk betweenness centrality for nodes by absorbing random walk, where the absorbing state is selected to be the destination node d [47, 30]. An extended analytical expression of random walk betweenness centrality for interconnected multilayer networks can be found in [29].

3.2.3 Random walk closeness centrality

A variant of closeness centrality is random walk closeness centrality, the computation of which is based on the mean first-passage time (MFPT). The MFPT is defined as the average number of steps to reach node d starting from a given node s . The lower average MFPT indicates that a node is on average more quickly accessible from other nodes. Therefore, a node with a lower average MFPT to all other nodes is considered more “central” in the network. The random walk closeness centrality is defined as the reciprocal of the average MFPT, and it is calculated by the formula:

$$C_{rwcc}(v) = \frac{n-1}{\sum_{u \in V \setminus \{v\}} \tau_{uv}}, \quad (14)$$

where τ_{uv} is the MFPT from node u to node v . The MFPT matrix can be calculated analytically by means of Kemeny-Snell fundamental matrix Z [50, 51] or by means of absorbing random walks [52, 47].

The analytical expressions of random walk closeness centrality in interconnected multilayer networks can be found in [29].

3.3 Game-theoretic centrality measures

3.3.1 Shapley value based centrality

The Shapley value is a solution concept in cooperative game theory introduced by Lloyd Shapley in 1953 [32]. It is a measure of the average marginal contribution of a player to all possible coalitions. Shapley value is a solution concept assigning a singleton solution to the players as allocation given by formula:

$$\phi(i) = \sum_{S \subseteq N \setminus \{i\}} \frac{|S|!(n-|S|-1)!}{n!} (v(S \cup \{i\}) - v(S)), \quad (15)$$

where $S \subseteq V$ represents a coalition, the value of coalition S can be denoted by $v(S)$. We define characteristic function $v(S)$ as half of the sum of the weighted degrees of all nodes in the subgraph induced by S , that is,

$$v(S) = \frac{1}{2} \sum_{\{i,j\} \subseteq S} W(i,j), \quad (16)$$

where $W(i,j)$ is the weight of the edge between nodes i and j within the subgraph induced by S , coefficient $\frac{1}{2}$ is used for correction in case of an undirected graph, each edge is counted twice when summing up over all pairs of nodes.

Algorithm 1 describes how to calculate the Shapley value based on a weighted graph. However, the Shapley value is computationally expensive, especially, for large networks with the large number of coalitions.³ Therefore, we propose a new approach to calculate an approximated Shapley value described in the next section.

3.3.2 Approximated Shapley value

According to the fact that the influence from other nodes is decreasing with an increase of the path length, we propose several ideas to fasten the calculation of the Shapley value:

1. *Depth limitation*: By limiting the depth of the reachable nodes considered, the number of subsets that need to be considered is reduced.
2. *Local subset iteration*: Iterating over subsets only within the reachable nodes, rather than the entire graph, decreases the number of iterations.
3. *Neighbor size sampling*: For a large number of neighbors, computational complexity can be reduced by random sampling, thereby decreasing the number of subsets iterated over.

³For a network with n nodes, the total number of coalitions is equal to 2^n .

Algorithm 1 Calculation of the Shapley Values based on weighted graph

Require: A graph $G(V, E, W)$ with $n = |V|$ nodes
Ensure: Shapley value component $\phi(i)$ for each node $i \in V$

- 1: **for all** nodes $i \in V$ **do**
- 2: Initialize $\phi(i) \leftarrow 0$
- 3: **end for**
- 4: **for all** nodes $i \in V$ **do**
- 5: **for all** subsets $S \subseteq V \setminus \{i\}$ **do**
- 6: Compute $v(S) \leftarrow \sum_{\{j,k\} \subseteq S} W(j,k)$ within subgraph induced by S
- 7: Compute $v(S \cup \{i\})$ within subgraph induced by $S \cup \{i\}$
- 8: $\Delta v(S, i) \leftarrow v(S \cup \{i\}) - v(S)$
- 9: coeff $\leftarrow \frac{|S|! \cdot (n - |S| - 1)!}{n!}$
- 10: $\phi(i) \leftarrow \phi(i) + \text{coeff} \cdot \Delta v(S, i)$
- 11: **end for**
- 12: **end for**

return $\phi(i)$ for all $i \in V$

We first define $\psi(i, d_{max})$ as the set of reachable nodes of node i up to given depth d_{max} excluding node i . We can calculate an approximated Shapley value of node i based on set $\psi(i, d_{max})$ by formula:

$$\phi_a(i) = \begin{cases} \sum_{S \subseteq \psi(i, d_{max})} \frac{v(S \cup \{i\}) - v(S)}{2^{|\psi(i, d_{max})|}} & \text{if } |\psi(i, d_{max})| < m, \\ \beta \sum_{S \subseteq \psi(i, d_{max})} \frac{v(S \cup \{i\}) - v(S)}{2^{|\psi(i, d_{max})|}} & \text{if } |\psi(i, d_{max})| \geq m, \end{cases} \quad (17)$$

where $\beta = \frac{|\psi(i, d_{max})| + 1}{m + 1}$ is a scaling factor, and m is the maximal number of reachable nodes considered.

For $|\psi(i, d_{max})| \geq m$, we create a random sample of m nodes from set $\psi(i, d_{max})$ several times and calculate the components of the Shapley value based on these samples. The sampling time $H_{|\psi(i, d_{max})|, m}$ is given by formula (18) (see [53]):

$$H_{|\psi(i, d_{max})|, m} = \left(\frac{|\psi(i, d_{max})| + \frac{1}{2}}{m} - \frac{1}{2} \right) (\ln |\psi(i, d_{max})| + \gamma) + \frac{1}{2}, \quad (18)$$

where $\gamma \approx 0.5772156649$ is the Euler-Mascheroni constant. This formula is the mathematical expectation of the number of samples for collecting m nodes from set $\psi(i, d_{max})$ until all reachable nodes are collected.⁴

Equation (17) gives a good approximation of the Shapley value, especially when the density of the graph is not very high (less than 0.7). We should highlight that our algorithm provide an accurate estimation of the ratio of the approximated component of the Shapley value to the sum of all its components. Knowing this ratio and exact value $v(N)$, it is easy to calculate the approximated Shapley value using the scaling factor ξ :

$$\xi = \frac{v(N)}{\sum_{i \in V} \phi_a(i)}. \quad (19)$$

The steps of calculation of the approximated Shapley value in weighted graphs is described in Algorithm 2. We use the same characteristic function as in the original Shapley value calculation, but we reduce the number of calculations following the ideas listed above.

We can get a more accurate approximated Shapley value by multiplying its components $\phi_a(i)$ given by equation (17) with factor ξ defined by (19). We include this step in the benchmark of Algorithm 2. The results of its work are presented in Section 4.1.

3.3.3 Myerson value based centrality

The Myerson value was introduced by Roger Myerson in 1977 [33], and it is an allocation rule when players are connected by a network structure. By modifying the calculation method of the Shapley value, Myerson takes into account connections in the network, thereby reflecting the influence of network structure on the cooperative game. Consider a game where graph G is a tree, which consists on N nodes and characteristic function is determined by the

⁴We can consider this problem as the generalized coupon collector's problem [53].

Algorithm 2 Calculation of approximated Shapley Value in weighted graph

Require: A weighted graph $G = (V, E, W)$, depth limit d_{max} , maximal size m of the set of reachable considered

Ensure: Approximated Shapley value $(\phi_a(i), i \in V)$

```

1: Initialize  $\phi_a(i) \leftarrow 0$  for each  $i \in V$ 
2: for  $i \in V$  do
3:    $\psi(i, d_{max}) \leftarrow$  Calculate or retrieve all reachable nodes of  $i$  up to depth  $d_{max}$ 
4:   if  $|\psi(i, d_{max})| < m$  then
5:     for each subset  $S \subseteq \psi(i, d_{max}) \setminus \{i\}$  do
6:       Compute  $v(S) \leftarrow \sum_{\{j,k\} \subseteq S} W(j, k)$  within subgraph induced by  $S$ 
7:       Compute  $v(S \cup \{i\})$  within subgraph induced by  $S \cup \{i\}$ 
8:        $\Delta v(S, i) \leftarrow v(S \cup \{i\}) - v(S)$ 
9:        $\phi_a(i) \leftarrow \phi_a(i) + \Delta v(S, i)$ 
10:    end for
11:    coeff  $\leftarrow \frac{1}{2^{|\psi(i, d_{max})|}}$ 
12:     $\phi_a(i) \leftarrow \phi_a(i) \cdot$  coeff, normalize  $\phi_a(i)$  based on the number of subsets
13:  else
14:    Pick up  $m$  nodes randomly from  $\psi(i, d_{max})$  and repeat  $H_{|\psi(i, d_{max})|, m}$  times
15:    for  $i = 1$  to  $H_{|\psi(i, d_{max})|, m}$  do
16:       $s_{reachable} \leftarrow$  Randomly select a sample of  $m$  nodes from  $\psi(i, d_{max})$ ,
17:      for each subset  $S \subseteq s_{reachable} \setminus \{i\}$  do
18:        Calculate  $v(S)$  and  $v(S \cup \{i\})$  as before
19:         $\Delta v(S, i) \leftarrow v(S \cup \{i\}) - v(S)$ 
20:         $\phi_a(i) \leftarrow \phi_a(i) + \Delta v(S, i)$ 
21:      end for
22:    end for
23:    coeff  $\leftarrow 1/2^{|\psi(i, d_{max})|} / H_{|\psi(i, d_{max})|, m} \cdot \frac{|\psi(i, d_{max})| + 1}{m + 1}$ 
24:     $\phi_a(i) \leftarrow \phi_a(i) \cdot$  coeff
25:  end if
26: end for
27: Define scaling factor  $\xi \leftarrow \frac{v(N)}{\sum_{i \in V} \phi_a(i)}$  ▷ For accurate results
28: return  $\phi_a(i) \leftarrow \xi \cdot \phi_a(i)$  for all  $i \in V$ 

```

scheme proposed in [54]. Every direct connection gives to coalition S a value r , where $0 \leq r \leq 1$. Players also obtain an impact from non-direct connections. This kind of impact will decrease with the increase of the path length. The characteristic function is defined as follows [35]:

$$v(S) = a_1 r + a_2 r^2 + \dots + a_k r^k + \dots + a_L r^L = \sum_{k=1}^L a_k r^k, \quad (20)$$

where L is a maximal distance between two nodes in the coalition; a_k is the number of paths of length k in this coalition; $v(i) = 0, \forall i \in N$.

Mazalov et al. in [55] proved that an allocation rule, that is, the Myerson value for unweighted graphs:

$$Y_i(v, g) = \frac{\sigma_1(i)}{2} r + \frac{\sigma_2(i)}{3} r^2 + \dots + \frac{\sigma_L(i)}{L+1} r^L = \sum_{k=1}^L \frac{\sigma_k(i)}{k+1} r^k, \quad (21)$$

where $\sigma_k(i)$ is a number of the paths of the length k including node i . The same approach to define an allocation can be applied to weighted graphs by converting the weight of the edge to the number of paths between two nodes, i.e. by converting a weighted graph to a multigraph [35].

3.3.4 Approximated Myerson value

However, calculation of the Myerson value is also computationally expensive, especially, for large networks. We can consider the rule of “six degrees separation” [56], implementing the idea that any two persons in the world who do not know each other only need a few intermediaries to establish a contact. Based on this idea, we can reduce the computational expense by limiting the maximal depth L of nodes with whom the node is connected. For a social

network, the higher the density, the lower intermediate nodes are needed to connect two nodes. We redefine L as follows:

$$L = \begin{cases} 6, & \text{if } D \leq 0.2, \\ 2, & \text{if } 0.2 < D \leq 0.3, \\ 1, & \text{if } D > 0.3, \end{cases} \quad (22)$$

where D is the density of the network.

The algorithm for calculation of Myerson values in weighted graphs is presented in Algorithm 3. We use the same characteristic function as given by equation 21, but we cutoff the maximal depth to approximate the Myerson value given by formula (22).

Algorithm 3 Calculation of the approximated Myerson value for weighted graph

Require: A weighted graph $G(V, E, W)$, discount factor r (default 0.5), boolean *weight* for considering edge weights (default True), boolean *approximate* for approximation (default True), boolean *scale* for scaling (default False)

Ensure: Components of Myerson value $Y_i(v, g)$, $i \in V$

```

1:  $Y_i(v, g) \leftarrow 0$  for each  $i \in V$  ▷ Initialize Myerson values
2: if approximate then
3:    $L \leftarrow \begin{cases} 1, & \text{if } \text{density}(G) > 0.3, \\ 2, & \text{if } \text{density}(G) > 0.2, \\ 6, & \text{otherwise} \end{cases}$  ▷ Adjust  $L$  based on  $\text{density}(G)$ .
4: else
5:    $L \leftarrow |V| - 1$  ▷ Without approximation
6: end if
7: for all  $i \in V$  do
8:    $l2c \leftarrow$  Initialize a length->count map for paths through  $i$ 
9:   for all pairs  $(start, end)$  in  $V \times V$  do
10:    for all  $path$  in all simple paths from  $start$  to  $end$  with  $length \leq L$  do
11:     if  $node \in path$  then
12:       $length \leftarrow \text{len}(path) - 1$ 
13:      if weight then
14:        $l2c[length] \leftarrow l2c[length] + \min_{(u,v) \in path} w(u, v)$ 
15:      else
16:        $l2c[length] \leftarrow l2c[length] + 1$ 
17:      end if
18:     end if
19:    end for
20:   end for
21:   for all  $(length, count) \in l2c$  do
22:     $count \leftarrow count/2$  ▷ Correct for double counting
23:     $Y_i(v, g) \leftarrow Y_i(v, g) + \left( count \cdot \frac{r^{length}}{length+1} \right)$ 
24:   end for
25: end for
26: if scale then
27:   Define  $\xi \leftarrow \frac{v(N)}{\sum_{i \in V} Y_i(v, g)}$  ▷ For more accurate results
28:   return  $Y_i(v, g) \leftarrow \xi \cdot Y_i(v, g)$  for all  $i \in V$ 
29: else
30:   return  $Y_i(v, g)$  for all  $i \in V$ 
31: end if

```

Similarly to equation (19), we can also define the scaling factor ξ for the approximated Myerson value as follows:

$$\xi = \frac{v(N)}{\sum_{i \in V} Y_i(v, g)}. \quad (23)$$

In both formulae (19) and (23), $v(N)$ is used, and to calculate it for the Myerson value we need to count the number of paths for all lengths, i.e. a_1, a_2, \dots, a_L . It is much more computationally expensive than in the case of the Shapley value. But after the ξ scaling, we obtain a more accurate approximation which will be shown in Section 4.1.

4 Experiments

Network structure has a huge impact on key performance indicators (KPIs) of opinion dynamics realized on this network. Therefore, we define several characteristics of a network which, in our opinion, have most significant correlation with KPIs of opinion dynamics. Our experiments are organized as follows: in Section 4.1 we provide the series of experiments in which we calculated the centralities based on approximated Shapley and Myerson values (realizations of Algorithms 2 and 3) for the graphs with varying density. We analyze correlation between KPIs of opinion dynamics and network properties in Section 4.2.

4.1 Centralities based on the Shapley and Myerson values

Due to the computational complexity of the Shapley value and Myerson value, we run our experiments on networks composed by 20 nodes for a given density. We create a network as follows: randomly and repeatedly take two different nodes from the set of nodes and add a connection between them until the density reaches a desired value. We designed the following experiments to evaluate the performance of the proposed centrality measures:

1. **Shapley-value based centrality:** The density of a network takes the values: 0.1, 0.2, \dots , 1.0. For each weighted or unweighted graph, we calculate the exact Shapley value and an approximated Shapley value. We compare (i) these two values and (ii) computation time for these two methods.
2. **Myerson-value based centrality:** The density of a network takes the values: 0.1, 0.11, \dots , 0.2.⁵ For each weighted or unweighted graph, we calculate the exact Myerson value and an approximated Myerson value. We compare: (i) these two values and (ii) computation time for these two methods. We also make the series of experiments on networks composed by 10 nodes with density from 0.05 to 1.0 to show efficiency of our algorithm to approximate the Myerson value.
3. **Comparison with classical centrality measures:** Based on the real social network dataset “Zachary’s karate club”, we created a two-layer network by adding different internal network structures. We reduce a two-layer network to a one-layer weighted network using opinion dynamics parameters by the method described in Section 2.4. The most important nodes in the network are nodes 0 (instructor — Mr Hi) and 33 (manager — John A). We define the coefficient of accuracy or simply accuracy of centrality measures as follows:

$$Ac = \frac{|\text{Top 2 nodes according to a centrality measure} \cap \{0, 33\}|}{2} \cdot 100\%. \quad (24)$$

The meaning of Ac is the percentage of important nodes (0 and 33) in the top two nodes identified by considered centrality measures. We also compare the accuracy Ac of the proposed centrality measures with the accuracy Ac of classical centrality measures (betweenness and closeness centralities).

The results of this part of experiments are presented in Tables 1–8. In Table 1 we provide the results for the graphs with 20 nodes and different density (from 0.1 to 1.0), weighted and unweighted graphs. We compare the computation time for the exact Shapley value (column “SV time”) and for an approximated Shapley value (column “ASV time”). In Table 1 we also present a root mean square error for an approximated Shapley value (column “RMSE ASV”) and for the ratio of the approximated Shapley value component to the sum of all its components (column “RMSE ratio ASV”). The lower the value of RMSE, the more accurate approximation we obtain. We can make the following conclusions based on the results from Table 1:

1. The computation time of an approximated Shapley value is much faster than the time of the exact Shapley value (see columns “SV time” and “ASV time”).
2. The root mean square error of the approximated Shapley value is very small (see column “RMSE ASV”), and root mean square error of the ratio is even smaller than the first one (see column “RMSE ratio ASV”). The ratio here is referred to the normalized values. The RMSE of ratio is the RMSE between the exact normalized Shapley values and the approximated normalized Shapley values. RMSE increases with an increase of the graph density because of the sampling procedure.
3. The weighted graph introduces greater uncertainty in the sampling process when graph density is high (≥ 0.7), leading to a slightly higher RMSE. However, even in the worst case (see graph “20-1.0” in Table 1), our algorithm still demonstrates a high accuracy.

⁵We limit the density to the set $\{0.1, 0.11, \dots, 0.2\}$ because even a small increase in density significantly increases computation time. This makes the realization of the series of experiments quite complicated.

Table 1: Results on the Shapley value when ξ scaling factor is applied

Graph	Weighted	SV time	ASV time	RMSE ASV	RMSE ratio ASV
20-0.1	True	$7.2 \cdot 10^2$	$2.2 \cdot 10^{-3}$	$2.6 \cdot 10^{-22}$	$5.5 \cdot 10^{-27}$
20-0.2	True	$8.7 \cdot 10^2$	$1.9 \cdot 10^{-2}$	$3.1 \cdot 10^{-22}$	$5.6 \cdot 10^{-27}$
20-0.3	True	$1 \cdot 10^3$	$1.5 \cdot 10^{-1}$	$1.6 \cdot 10^{-22}$	$1.2 \cdot 10^{-27}$
20-0.4	True	$1.2 \cdot 10^3$	$9.3 \cdot 10^{-1}$	$1.7 \cdot 10^{-22}$	$6.1 \cdot 10^{-28}$
20-0.5	True	$1.3 \cdot 10^3$	$2.2 \cdot 10^0$	$7.1 \cdot 10^{-23}$	$2 \cdot 10^{-28}$
20-0.6	True	$1.5 \cdot 10^3$	$1.9 \cdot 10^1$	$7.7 \cdot 10^{-23}$	$1.8 \cdot 10^{-28}$
20-0.7	True	$1.6 \cdot 10^3$	$4.7 \cdot 10^1$	$3.3 \cdot 10^{-2}$	$6 \cdot 10^{-8}$
20-0.8	True	$1.7 \cdot 10^3$	$1.7 \cdot 10^2$	$2 \cdot 10^0$	$2.9 \cdot 10^{-6}$
20-0.9	True	$1.8 \cdot 10^3$	$2.5 \cdot 10^2$	$6.9 \cdot 10^0$	$7.9 \cdot 10^{-6}$
20-1.0	True	$1.9 \cdot 10^3$	$3.2 \cdot 10^2$	$9.9 \cdot 10^0$	$9 \cdot 10^{-6}$
20-0.1	False	$7.2 \cdot 10^2$	$3.4 \cdot 10^{-3}$	$4.5 \cdot 10^{-23}$	$1.1 \cdot 10^{-26}$
20-0.2	False	$8.8 \cdot 10^2$	$1.6 \cdot 10^{-2}$	$1.1 \cdot 10^{-22}$	$7.8 \cdot 10^{-27}$
20-0.3	False	$1 \cdot 10^3$	$9.6 \cdot 10^{-2}$	$1.1 \cdot 10^{-22}$	$6.6 \cdot 10^{-27}$
20-0.4	False	$1.2 \cdot 10^3$	$5.5 \cdot 10^{-1}$	$1.5 \cdot 10^{-22}$	$1.6 \cdot 10^{-26}$
20-0.5	False	$1.3 \cdot 10^3$	$2.9 \cdot 10^0$	$1.1 \cdot 10^{-22}$	$8.6 \cdot 10^{-27}$
20-0.6	False	$1.5 \cdot 10^3$	$2.5 \cdot 10^1$	$1.4 \cdot 10^{-22}$	$9.4 \cdot 10^{-27}$
20-0.7	False	$1.6 \cdot 10^3$	$6.2 \cdot 10^1$	$3.8 \cdot 10^{-4}$	$2.1 \cdot 10^{-8}$
20-0.8	False	$1.7 \cdot 10^3$	$1.7 \cdot 10^2$	$1.8 \cdot 10^{-3}$	$7.7 \cdot 10^{-8}$
20-0.9	False	$1.8 \cdot 10^3$	$2.5 \cdot 10^2$	$2 \cdot 10^{-3}$	$6.9 \cdot 10^{-8}$
20-1.0	False	$1.9 \cdot 10^3$	$3.2 \cdot 10^2$	$4.1 \cdot 10^{-21}$	$8.6 \cdot 10^{-34}$

In Tables 2 and 3 we present the results on computation of the Myerson value (exact and approximated) without and with scaling factor ξ defined by (23), respectively. In both tables we provide the results for the graphs with 20 nodes and different density (from 0.1 to 0.2), weighted and unweighted graphs. We compare the computation time for the exact Myerson value (column “MV time”) and for an approximated Myerson value (column “AMV time”). In these two tables we also present a root mean square error for an approximated Myerson value (column “RMSE AMV”) and for the ratio of the approximated Myerson value component to the sum of all its components (column “RMSE ratio AMV”). Conclusions from Tables 2 and 3 are

1. The computational complexity of the exact Myerson-value based centrality grows rapidly with the increase of the network density (column “MV time”).
2. The root mean square error of an approximated Myerson value grows with an increase of the network density (see column “RMSE AMV”), but the root mean square error of the ratio is very small. The RMSE of the ratio means the RMSE between the normalized approximated and normalized exact Myerson values. Therefore, we can recommend to use an approximation of the Myerson value as an approximated centrality measure.
3. If we estimate the effect of scaling factor ξ on the results, we can compare “AMV time” in Tables 2 and 3, and conclude that without ξ the computation time is much smaller, but the RMSE AMV is higher. While the RMSE ratio AMV between Tables 2 and 3 are almost the same.
4. Comparing Tables 2 and 3, we cannot see a significant difference in the results referred to weighted and unweighted graphs.

Next, we demonstrate the efficiency of our algorithm to approximate the Myerson value in high-density graphs. To do this, we examine graphs with 10 nodes and with density from 0.05 to 1.0 with step 0.05, weighted and unweighted graphs. The results of our experiments are presented in Tables 4 and 5 for the cases without and with scaling factor, respectively.

By comparing the pairs of Tables 2 and 3, and Tables 4 and 5, we can conclude that the scaling factor ξ has a very limited effect on reducing the error of an approximated Myerson value and moreover using ξ significantly increases computation time. But the RMSE of ratio is very small. Therefore, we could recommend to use the Myerson-value based centrality approximation without scaling factor ξ and better its ratio as an approximation of the Myerson value.

In Table 1, the results for the weighted graph with density 1.0 show the highest RMSE, and in Table 3 the results for the weighted graph with density 0.2 also show the highest RMSE. Therefore, we decide to carefully examine the high-density case and examine the Shapley value for the weighted graph with density 1.0 and the Myerson value for the weighted graph with density 0.2. To make analysis, we show the components of the exact and approximated Shapley values in Table 6 for the former graph and the exact and approximated Myerson values in Table 7 for the latter graph. In these tables we provide a relative error which is calculated by taking the difference between the approximated value and the exact value dividing this difference by the exact value, that is, $\frac{\text{approximated value} - \text{exact value}}{\text{exact value}}$.

Table 2: Results on the Myerson value without ξ scaling

Graph	Weighted	MV time	AMV time	RMSE AMV	RMSE ratio AMV
20-0.1	True	$1.03 \cdot 10^{-1}$	$1.62 \cdot 10^{-1}$	$4.37 \cdot 10^{-4}$	$1.48 \cdot 10^{-8}$
20-0.11	True	$1.91 \cdot 10^{-1}$	$1.67 \cdot 10^{-1}$	$8.75 \cdot 10^{-4}$	$1.7 \cdot 10^{-8}$
20-0.12	True	$4.17 \cdot 10^{-1}$	$2.23 \cdot 10^{-1}$	$1.54 \cdot 10^{-1}$	$5.28 \cdot 10^{-7}$
20-0.13	True	$1.02 \cdot 10^0$	$3.56 \cdot 10^{-1}$	$5.28 \cdot 10^{-1}$	$8.15 \cdot 10^{-7}$
20-0.14	True	$2.21 \cdot 10^0$	$6.15 \cdot 10^{-1}$	$2.14 \cdot 10^0$	$1.93 \cdot 10^{-6}$
20-0.15	True	$8.78 \cdot 10^0$	$9.24 \cdot 10^{-1}$	$1.89 \cdot 10^1$	$4.3 \cdot 10^{-6}$
20-0.16	True	$1.8 \cdot 10^1$	$1.48 \cdot 10^0$	$1.27 \cdot 10^2$	$1.25 \cdot 10^{-5}$
20-0.17	True	$2.87 \cdot 10^1$	$2.14 \cdot 10^0$	$4.06 \cdot 10^2$	$3.24 \cdot 10^{-5}$
20-0.18	True	$6.34 \cdot 10^1$	$2.77 \cdot 10^0$	$1.55 \cdot 10^3$	$4.7 \cdot 10^{-5}$
20-0.19	True	$1.45 \cdot 10^2$	$3.58 \cdot 10^0$	$4.82 \cdot 10^3$	$8.66 \cdot 10^{-5}$
20-0.2	True	$2.94 \cdot 10^2$	$4.45 \cdot 10^0$	$1.33 \cdot 10^4$	$1.35 \cdot 10^{-4}$
20-0.1	False	$3.3 \cdot 10^{-1}$	$1.96 \cdot 10^{-1}$	$1.12 \cdot 10^{-2}$	$1.43 \cdot 10^{-6}$
20-0.11	False	$3.45 \cdot 10^{-1}$	$2.16 \cdot 10^{-1}$	$1.73 \cdot 10^{-2}$	$1.41 \cdot 10^{-6}$
20-0.12	False	$4.87 \cdot 10^{-1}$	$2.17 \cdot 10^{-1}$	$3.43 \cdot 10^{-2}$	$1.52 \cdot 10^{-6}$
20-0.13	False	$1.37 \cdot 10^0$	$3.79 \cdot 10^{-1}$	$3.95 \cdot 10^{-1}$	$5.73 \cdot 10^{-6}$
20-0.14	False	$3.69 \cdot 10^0$	$5.81 \cdot 10^{-1}$	$2.71 \cdot 10^0$	$1.53 \cdot 10^{-5}$
20-0.15	False	$7.65 \cdot 10^0$	$1.05 \cdot 10^0$	$1.38 \cdot 10^1$	$2.75 \cdot 10^{-5}$
20-0.16	False	$1.71 \cdot 10^1$	$1.38 \cdot 10^0$	$5.94 \cdot 10^1$	$4.19 \cdot 10^{-5}$
20-0.17	False	$4.28 \cdot 10^1$	$1.62 \cdot 10^0$	$2.97 \cdot 10^2$	$6.29 \cdot 10^{-5}$
20-0.18	False	$8.25 \cdot 10^1$	$1.88 \cdot 10^0$	$8.04 \cdot 10^2$	$6.73 \cdot 10^{-5}$
20-0.19	False	$1.69 \cdot 10^2$	$2.56 \cdot 10^0$	$2.72 \cdot 10^3$	$7.6 \cdot 10^{-5}$
20-0.2	False	$3.66 \cdot 10^2$	$3.57 \cdot 10^0$	$8.75 \cdot 10^3$	$1.31 \cdot 10^{-4}$

 Table 3: Results on the Myerson value when ξ scaling is applied

Graph	Weighted	MV time	AMV time	RMSE AMV	RMSE ratio AMV
20-0.1	True	$1.23 \cdot 10^{-1}$	$1.1 \cdot 10^{-1}$	$1.98 \cdot 10^{-4}$	$1.48 \cdot 10^{-8}$
20-0.11	True	$1.57 \cdot 10^{-1}$	$2.11 \cdot 10^{-1}$	$3.21 \cdot 10^{-4}$	$1.7 \cdot 10^{-8}$
20-0.12	True	$4.53 \cdot 10^{-1}$	$2.21 \cdot 10^{-1}$	$1.55 \cdot 10^{-2}$	$5.28 \cdot 10^{-7}$
20-0.13	True	$9.1 \cdot 10^{-1}$	$4.33 \cdot 10^{-1}$	$3.15 \cdot 10^{-2}$	$8.15 \cdot 10^{-7}$
20-0.14	True	$2.09 \cdot 10^0$	$6.7 \cdot 10^{-1}$	$1.08 \cdot 10^{-1}$	$1.93 \cdot 10^{-6}$
20-0.15	True	$7.83 \cdot 10^0$	$1.24 \cdot 10^0$	$4.81 \cdot 10^{-1}$	$4.3 \cdot 10^{-6}$
20-0.16	True	$1.65 \cdot 10^1$	$2.24 \cdot 10^0$	$3.85 \cdot 10^0$	$1.25 \cdot 10^{-5}$
20-0.17	True	$2.63 \cdot 10^1$	$3.28 \cdot 10^0$	$2.36 \cdot 10^1$	$3.24 \cdot 10^{-5}$
20-0.18	True	$5.91 \cdot 10^1$	$5.91 \cdot 10^0$	$6.15 \cdot 10^1$	$4.7 \cdot 10^{-5}$
20-0.19	True	$1.41 \cdot 10^2$	$1.15 \cdot 10^1$	$2.07 \cdot 10^2$	$8.66 \cdot 10^{-5}$
20-0.2	True	$2.92 \cdot 10^2$	$2.06 \cdot 10^1$	$6.48 \cdot 10^2$	$1.35 \cdot 10^{-4}$
20-0.1	False	$2.75 \cdot 10^{-1}$	$2.43 \cdot 10^{-1}$	$1.59 \cdot 10^{-3}$	$1.43 \cdot 10^{-6}$
20-0.11	False	$3.64 \cdot 10^{-1}$	$1.94 \cdot 10^{-1}$	$1.81 \cdot 10^{-3}$	$1.41 \cdot 10^{-6}$
20-0.12	False	$4.56 \cdot 10^{-1}$	$2.47 \cdot 10^{-1}$	$2.65 \cdot 10^{-3}$	$1.52 \cdot 10^{-6}$
20-0.13	False	$1.34 \cdot 10^0$	$4.13 \cdot 10^{-1}$	$2.01 \cdot 10^{-2}$	$5.73 \cdot 10^{-6}$
20-0.14	False	$3.33 \cdot 10^0$	$6.97 \cdot 10^{-1}$	$1.18 \cdot 10^{-1}$	$1.53 \cdot 10^{-5}$
20-0.15	False	$7.17 \cdot 10^0$	$1.29 \cdot 10^0$	$5.64 \cdot 10^{-1}$	$2.75 \cdot 10^{-5}$
20-0.16	False	$1.55 \cdot 10^1$	$2.01 \cdot 10^0$	$1.92 \cdot 10^0$	$4.19 \cdot 10^{-5}$
20-0.17	False	$3.93 \cdot 10^1$	$3.3 \cdot 10^0$	$7.44 \cdot 10^0$	$6.29 \cdot 10^{-5}$
20-0.18	False	$7.78 \cdot 10^1$	$5.58 \cdot 10^0$	$1.6 \cdot 10^1$	$6.73 \cdot 10^{-5}$
20-0.19	False	$1.64 \cdot 10^2$	$1.06 \cdot 10^1$	$4.58 \cdot 10^1$	$7.6 \cdot 10^{-5}$
20-0.2	False	$3.43 \cdot 10^2$	$1.99 \cdot 10^1$	$2.06 \cdot 10^2$	$1.31 \cdot 10^{-4}$

Table 4: Results on the Myerson value without ξ scaling for networks with 10 nodes

Graph	Weighted	MV time	AMV time	RMSE AMV	RMSE ratio AMV
10-0.05	True	$1.24 \cdot 10^{-3}$	$1.59 \cdot 10^{-2}$	$0 \cdot 10^0$	$0 \cdot 10^0$
10-0.1	True	$1.79 \cdot 10^{-3}$	$1.58 \cdot 10^{-3}$	$0 \cdot 10^0$	$0 \cdot 10^0$
10-0.15	True	$1.27 \cdot 10^{-2}$	$3.17 \cdot 10^{-3}$	$0 \cdot 10^0$	$0 \cdot 10^0$
10-0.2	True	$7.33 \cdot 10^{-3}$	$1.05 \cdot 10^{-2}$	$9.65 \cdot 10^{-6}$	$7.63 \cdot 10^{-10}$
10-0.25	True	$1.49 \cdot 10^{-2}$	$2.89 \cdot 10^{-3}$	$3.27 \cdot 10^1$	$1.64 \cdot 10^{-4}$
10-0.3	True	$6.69 \cdot 10^{-2}$	$3.35 \cdot 10^{-3}$	$2.79 \cdot 10^2$	$1.91 \cdot 10^{-4}$
10-0.35	True	$1.17 \cdot 10^{-1}$	$1.78 \cdot 10^{-3}$	$1.85 \cdot 10^3$	$5.12 \cdot 10^{-4}$
10-0.4	True	$2.6 \cdot 10^{-1}$	$1.2 \cdot 10^{-3}$	$4.58 \cdot 10^3$	$4.08 \cdot 10^{-4}$
10-0.45	True	$5.53 \cdot 10^{-1}$	$1.21 \cdot 10^{-3}$	$1.05 \cdot 10^4$	$6.26 \cdot 10^{-4}$
10-0.5	True	$1.21 \cdot 10^0$	$1.37 \cdot 10^{-3}$	$1.56 \cdot 10^4$	$5.53 \cdot 10^{-4}$
10-0.55	True	$2.56 \cdot 10^0$	$1.26 \cdot 10^{-3}$	$3.92 \cdot 10^4$	$4.49 \cdot 10^{-4}$
10-0.6	True	$5.7 \cdot 10^0$	$1.62 \cdot 10^{-3}$	$1.11 \cdot 10^5$	$6.17 \cdot 10^{-4}$
10-0.65	True	$1.05 \cdot 10^1$	$1.33 \cdot 10^{-3}$	$2.31 \cdot 10^5$	$7.47 \cdot 10^{-4}$
10-0.7	True	$1.99 \cdot 10^1$	$1.33 \cdot 10^{-3}$	$5.19 \cdot 10^5$	$6.84 \cdot 10^{-4}$
10-0.75	True	$3.55 \cdot 10^1$	$6.44 \cdot 10^{-3}$	$1 \cdot 10^6$	$5.96 \cdot 10^{-4}$
10-0.8	True	$7.36 \cdot 10^1$	$1.38 \cdot 10^{-3}$	$3.42 \cdot 10^6$	$5.9 \cdot 10^{-4}$
10-0.85	True	$1.15 \cdot 10^2$	$1.38 \cdot 10^{-3}$	$8.11 \cdot 10^6$	$3.76 \cdot 10^{-4}$
10-0.9	True	$1.73 \cdot 10^2$	$1.39 \cdot 10^{-3}$	$1.63 \cdot 10^7$	$3.92 \cdot 10^{-4}$
10-0.95	True	$2.48 \cdot 10^2$	$1.37 \cdot 10^{-3}$	$2.74 \cdot 10^7$	$3.7 \cdot 10^{-4}$
10-1.0	True	$4.33 \cdot 10^2$	$1.37 \cdot 10^{-3}$	$7.31 \cdot 10^7$	$2.79 \cdot 10^{-4}$
10-0.05	False	$1.15 \cdot 10^{-3}$	$1.06 \cdot 10^{-3}$	$0 \cdot 10^0$	$0 \cdot 10^0$
10-0.1	False	$2.09 \cdot 10^{-3}$	$1.99 \cdot 10^{-3}$	$0 \cdot 10^0$	$0 \cdot 10^0$
10-0.15	False	$3.4 \cdot 10^{-3}$	$2.84 \cdot 10^{-3}$	$0 \cdot 10^0$	$0 \cdot 10^0$
10-0.2	False	$7.57 \cdot 10^{-3}$	$1.08 \cdot 10^{-2}$	$0 \cdot 10^0$	$0 \cdot 10^0$
10-0.25	False	$3.14 \cdot 10^{-2}$	$8.37 \cdot 10^{-3}$	$2.56 \cdot 10^0$	$1.57 \cdot 10^{-4}$
10-0.3	False	$3.12 \cdot 10^{-2}$	$3.11 \cdot 10^{-3}$	$8.85 \cdot 10^0$	$9.04 \cdot 10^{-5}$
10-0.35	False	$8.49 \cdot 10^{-2}$	$1.13 \cdot 10^{-3}$	$5.98 \cdot 10^1$	$1.53 \cdot 10^{-4}$
10-0.4	False	$2.18 \cdot 10^{-1}$	$1.33 \cdot 10^{-3}$	$2.28 \cdot 10^2$	$1.29 \cdot 10^{-4}$
10-0.45	False	$4.74 \cdot 10^{-1}$	$1.16 \cdot 10^{-3}$	$6.23 \cdot 10^2$	$9.58 \cdot 10^{-5}$
10-0.5	False	$9.61 \cdot 10^{-1}$	$1.17 \cdot 10^{-3}$	$1.81 \cdot 10^3$	$8.71 \cdot 10^{-5}$
10-0.55	False	$1.95 \cdot 10^0$	$1.21 \cdot 10^{-3}$	$4.91 \cdot 10^3$	$7.4 \cdot 10^{-5}$
10-0.6	False	$4.15 \cdot 10^0$	$1.3 \cdot 10^{-3}$	$1.97 \cdot 10^4$	$4.98 \cdot 10^{-5}$
10-0.65	False	$7.11 \cdot 10^0$	$1.24 \cdot 10^{-3}$	$4.79 \cdot 10^4$	$5.33 \cdot 10^{-5}$
10-0.7	False	$1.14 \cdot 10^1$	$1.33 \cdot 10^{-3}$	$1.07 \cdot 10^5$	$9.37 \cdot 10^{-5}$
10-0.75	False	$1.86 \cdot 10^1$	$3.51 \cdot 10^{-3}$	$2.46 \cdot 10^5$	$1.6 \cdot 10^{-4}$
10-0.8	False	$3.77 \cdot 10^1$	$1.39 \cdot 10^{-3}$	$8.53 \cdot 10^5$	$1.07 \cdot 10^{-4}$
10-0.85	False	$5.26 \cdot 10^1$	$1.29 \cdot 10^{-3}$	$1.73 \cdot 10^6$	$1.35 \cdot 10^{-4}$
10-0.9	False	$7.45 \cdot 10^1$	$1.31 \cdot 10^{-3}$	$3.64 \cdot 10^6$	$9.85 \cdot 10^{-5}$
10-0.95	False	$1.05 \cdot 10^2$	$1.3 \cdot 10^{-3}$	$7.74 \cdot 10^6$	$4.85 \cdot 10^{-5}$
10-1.0	False	$1.71 \cdot 10^2$	$1.28 \cdot 10^{-3}$	$2.16 \cdot 10^7$	$0 \cdot 10^0$

Analyzing Table 6, we can say that our algorithm provides a very accurate approximation for the Shapley value such that only for two nodes (Nodes 5 and 19) the absolute relative error is larger than 5%.

Analyzing the results in Table 7, we can find that some nodes (Nodes 1, 2, 8, and 9) have a high relative error in approximation. The reason is that in our algorithm we count the number of paths not for all lengths ($length \leq L$). By increasing L we can obtain a more accurate result, but it will increase the computational complexity.

The last item in analysis of this series of experiments is to compare the accuracy defined by (24) for the approximated Shapley and Myerson values, and for the classical centrality measures (betweenness and closeness). We summarize these results in Table 8. Both centrality measures proposed in this paper have a higher accuracy than the classical centrality measures. In particular, an approximated Shapley-value based centrality can identify the most important nodes with 100% accuracy for all examined graphs. For the approximated Myerson value based centrality, it has 100% accuracy for all cases except a case of a network “karate-twoStar-34”, for which the accuracy is 50%. The mistake in prediction of one of the most important nodes is that another node (Node 17) is the central one in the internal layer by construction. For the betweenness centrality, the accuracy is zero for high-density networks. Closeness centrality also has the worst accuracy for these networks.

4.2 Experiments to examine correlation of network properties and opinion dynamics

We have done simulations of opinion dynamics in one-layer Zachary’s karate club network following BVM and two-layer network following GCVN with Zachary’s karate club network being an external layer and different internal network structures. There is a list of internal layers we use in our analysis:

Table 5: Results on the Myerson value when ξ scaling is applied for networks with 10 nodes

Graph	Weighted	MV time	AMV time	RMSE AMV	RMSE ratio AMV
10-0.05	True	$1.24 \cdot 10^{-3}$	$1.22 \cdot 10^{-3}$	$0 \cdot 10^0$	$0 \cdot 10^0$
10-0.1	True	$3.08 \cdot 10^{-3}$	$1.99 \cdot 10^{-3}$	$6.24 \cdot 10^{-32}$	$0 \cdot 10^0$
10-0.15	True	$4.67 \cdot 10^{-3}$	$3.73 \cdot 10^{-3}$	$0 \cdot 10^0$	$0 \cdot 10^0$
10-0.2	True	$1.2 \cdot 10^{-2}$	$1.74 \cdot 10^{-2}$	$3.25 \cdot 10^{-6}$	$7.63 \cdot 10^{-10}$
10-0.25	True	$1.46 \cdot 10^{-2}$	$4.48 \cdot 10^{-3}$	$1.67 \cdot 10^0$	$1.64 \cdot 10^{-4}$
10-0.3	True	$4.97 \cdot 10^{-2}$	$8.24 \cdot 10^{-3}$	$6.05 \cdot 10^0$	$1.91 \cdot 10^{-4}$
10-0.35	True	$1.05 \cdot 10^{-1}$	$1.69 \cdot 10^{-2}$	$3.5 \cdot 10^1$	$5.12 \cdot 10^{-4}$
10-0.4	True	$2.57 \cdot 10^{-1}$	$2.63 \cdot 10^{-2}$	$6.41 \cdot 10^1$	$4.08 \cdot 10^{-4}$
10-0.45	True	$5.52 \cdot 10^{-1}$	$7.07 \cdot 10^{-2}$	$2.14 \cdot 10^2$	$6.26 \cdot 10^{-4}$
10-0.5	True	$1.18 \cdot 10^0$	$1.27 \cdot 10^{-1}$	$2.91 \cdot 10^2$	$5.53 \cdot 10^{-4}$
10-0.55	True	$2.5 \cdot 10^0$	$3.8 \cdot 10^{-1}$	$5.78 \cdot 10^2$	$4.49 \cdot 10^{-4}$
10-0.6	True	$5.81 \cdot 10^0$	$5.76 \cdot 10^{-1}$	$2.15 \cdot 10^3$	$6.17 \cdot 10^{-4}$
10-0.65	True	$1.06 \cdot 10^1$	$1.24 \cdot 10^0$	$5.36 \cdot 10^3$	$7.47 \cdot 10^{-4}$
10-0.7	True	$1.98 \cdot 10^1$	$2.14 \cdot 10^0$	$1.12 \cdot 10^4$	$6.84 \cdot 10^{-4}$
10-0.75	True	$3.57 \cdot 10^1$	$3.66 \cdot 10^0$	$1.9 \cdot 10^4$	$5.96 \cdot 10^{-4}$
10-0.8	True	$7.43 \cdot 10^1$	$6.77 \cdot 10^0$	$6.41 \cdot 10^4$	$5.9 \cdot 10^{-4}$
10-0.85	True	$1.16 \cdot 10^2$	$1.11 \cdot 10^1$	$9.71 \cdot 10^4$	$3.76 \cdot 10^{-4}$
10-0.9	True	$1.75 \cdot 10^2$	$1.71 \cdot 10^1$	$2.03 \cdot 10^5$	$3.92 \cdot 10^{-4}$
10-0.95	True	$2.48 \cdot 10^2$	$2.45 \cdot 10^1$	$3.22 \cdot 10^5$	$3.7 \cdot 10^{-4}$
10-1.0	True	$4.33 \cdot 10^2$	$4.33 \cdot 10^1$	$6.49 \cdot 10^5$	$2.79 \cdot 10^{-4}$
10-0.05	False	$1.23 \cdot 10^{-3}$	$1.29 \cdot 10^{-3}$	$0 \cdot 10^0$	$0 \cdot 10^0$
10-0.1	False	$2.28 \cdot 10^{-3}$	$2.55 \cdot 10^{-3}$	$0 \cdot 10^0$	$0 \cdot 10^0$
10-0.15	False	$4.91 \cdot 10^{-3}$	$1.73 \cdot 10^{-2}$	$0 \cdot 10^0$	$0 \cdot 10^0$
10-0.2	False	$2.15 \cdot 10^{-2}$	$7.96 \cdot 10^{-3}$	$2.16 \cdot 10^{-31}$	$2.65 \cdot 10^{-33}$
10-0.25	False	$1.64 \cdot 10^{-2}$	$9.18 \cdot 10^{-3}$	$5.35 \cdot 10^{-2}$	$1.57 \cdot 10^{-4}$
10-0.3	False	$4.56 \cdot 10^{-2}$	$6.48 \cdot 10^{-3}$	$7.23 \cdot 10^{-2}$	$9.04 \cdot 10^{-5}$
10-0.35	False	$6.45 \cdot 10^{-2}$	$6.84 \cdot 10^{-3}$	$3.23 \cdot 10^{-1}$	$1.53 \cdot 10^{-4}$
10-0.4	False	$2.43 \cdot 10^{-1}$	$1.99 \cdot 10^{-2}$	$1.02 \cdot 10^0$	$1.29 \cdot 10^{-4}$
10-0.45	False	$4.54 \cdot 10^{-1}$	$3.73 \cdot 10^{-2}$	$2 \cdot 10^0$	$9.58 \cdot 10^{-5}$
10-0.5	False	$9.12 \cdot 10^{-1}$	$8.23 \cdot 10^{-2}$	$5.1 \cdot 10^0$	$8.71 \cdot 10^{-5}$
10-0.55	False	$1.86 \cdot 10^0$	$2.11 \cdot 10^{-1}$	$1.15 \cdot 10^1$	$7.4 \cdot 10^{-5}$
10-0.6	False	$4.29 \cdot 10^0$	$3.61 \cdot 10^{-1}$	$3.03 \cdot 10^1$	$4.98 \cdot 10^{-5}$
10-0.65	False	$7.36 \cdot 10^0$	$6.8 \cdot 10^{-1}$	$7.83 \cdot 10^1$	$5.33 \cdot 10^{-5}$
10-0.7	False	$1.14 \cdot 10^1$	$1.51 \cdot 10^0$	$3.05 \cdot 10^2$	$9.37 \cdot 10^{-5}$
10-0.75	False	$1.94 \cdot 10^1$	$2.03 \cdot 10^0$	$1.23 \cdot 10^3$	$1.6 \cdot 10^{-4}$
10-0.8	False	$3.74 \cdot 10^1$	$3.41 \cdot 10^0$	$2.9 \cdot 10^3$	$1.07 \cdot 10^{-4}$
10-0.85	False	$5.27 \cdot 10^1$	$5.04 \cdot 10^0$	$7.35 \cdot 10^3$	$1.35 \cdot 10^{-4}$
10-0.9	False	$7.45 \cdot 10^1$	$6.5 \cdot 10^0$	$1.13 \cdot 10^4$	$9.85 \cdot 10^{-5}$
10-0.95	False	$1.05 \cdot 10^2$	$9.53 \cdot 10^0$	$1.19 \cdot 10^4$	$4.85 \cdot 10^{-5}$
10-1.0	False	$1.71 \cdot 10^2$	$1.63 \cdot 10^1$	$0 \cdot 10^0$	$0 \cdot 10^0$

Table 6: Exact Shapley value vs an approximated Shapley value for “graph-1.0”

Nodes	SV	SV ratio	ASV	ASV ratio	Rel. error ASV/SV
0	52.0000	4.96%	53.3579	5.09%	2.61%
1	46.5000	4.43%	46.5090	4.43%	$1.83 \cdot 10^{-2}\%$
2	50.5000	4.81%	49.0574	4.68%	-2.86%
3	53.0000	5.05%	53.6764	5.12%	1.28%
4	50.5000	4.81%	50.0131	4.77%	-0.96%
5	50.0000	4.77%	54.3135	5.18%	8.63%
6	50.0000	4.77%	51.2873	4.89%	2.57%
7	63.0000	6.01%	62.5960	5.97%	-0.64%
8	55.0000	5.24%	53.3579	5.09%	-2.98%
9	44.0000	4.19%	44.4384	4.24%	0.99%
10	49.5000	4.72%	50.3316	4.80%	1.68%
11	51.0000	4.86%	51.6058	4.92%	1.19%
12	64.0000	6.10%	62.9145	6.00%	-1.70%
13	49.0000	4.67%	49.0574	4.68%	0.12%
14	48.0000	4.58%	47.9425	4.57%	-0.12%
15	63.5000	6.05%	63.0738	6.01%	-0.67%
16	54.0000	5.15%	54.4728	5.19%	0.87%
17	57.0000	5.43%	57.0213	5.44%	$3.66 \cdot 10^{-2}\%$
18	53.0000	5.05%	52.0837	4.97%	-1.73%
19	45.5000	4.34%	41.8899	3.99%	-7.93%

Table 7: Exact Myerson value vs an approximated Myerson value for “graph-0.2”

Nodes	MV	MV ratio	AMV	AMV ratio	Rel. error AMV/MV
0	143.2672	6.53%	144.0222	6.56%	0.53%
1	68.7002	3.13%	49.3370	2.25%	-28.18%
2	68.0767	3.10%	81.6335	3.72%	19.91%
3	104.6799	4.77%	109.9763	5.01%	5.06%
4	164.0880	7.48%	157.1853	7.16%	-4.21%
5	114.6388	5.22%	106.1499	4.84%	-7.40%
6	16.7705	0.76%	17.8578	0.81%	6.48%
7	228.8444	10.43%	251.4307	11.46%	9.87%
8	33.7682	1.54%	24.3128	1.11%	-28.00%
9	36.1832	1.65%	28.1827	1.28%	-22.11%
10	184.1740	8.39%	192.6532	8.78%	4.60%
11	79.7901	3.64%	69.8602	3.18%	-12.45%
12	56.7906	2.59%	53.0066	2.42%	-6.66%
13	48.8678	2.23%	46.0495	2.10%	-5.77%
14	107.3196	4.89%	93.9069	4.28%	-12.50%
15	63.4039	2.89%	66.5861	3.03%	5.02%
16	186.6146	8.50%	200.2029	9.12%	7.28%
17	229.3778	10.45%	258.1879	11.77%	12.56%
18	162.6473	7.41%	152.4821	6.95%	-6.25%
19	96.4034	4.39%	91.3826	4.16%	-5.21%

Table 8: Accuracy defined by (24) for the proposed in this paper and classical centrality measures

graph \ accuracy	betweenness	closeness	Shapley value	Myerson value
karate-34	100%	50%	100%	100%
karate-empty-34	100%	50%	100%	100%
karate-karate-34	100%	50%	100%	100%
karate-star-34	100%	100%	100%	100%
karate-twoStar-34	100%	50%	100%	50%
karate-cycle-34	100%	100%	100%	100%
karate-twoClique-34	0%	0%	100%	100%
karate-complete-34	0%	0%	100%	100%

1. **karate**: Zachary’s karate club network;
2. **star**: star structure with node 0 being the center;
3. **two-star**: two central nodes 0 and 17, nodes 1–16 are linked with node 0, nodes 18–33 are linked with node 17. Moreover, nodes 0 and 17 are linked;
4. **cycle**: node 0 is linked with node 1, node 1 is linked with node 2, and so on. Finally, node 33 is linked with node 0;
5. **two-clique**: nodes 0–16 belong to the first clique, nodes 17–33 — to the second clique, and these two cliques are connected through link between nodes 0 and 17;
6. **complete**: all nodes are linked with each other.

We start with simulations of opinion dynamics of BVM for one-layer network, and then CVM and GVM for two-layer networks implementing different internal structures and examine their affect on consensus time and winning rate. Network properties (in this work, centrality measures) will also change with changes of the network structure.

We describe the results of our experiments:

- Fig. 3a shows how internal average shortest path d_I varies depending on the network structure.⁶
- Fig. 3b shows how internal density varies depending on the network structure. By comparing Fig. 3a and 3b, we can notice that the internal density D_I and internal average shortest path d_I are negatively correlated.
- Fig. 4 shows different centralities for Nodes 0 and 33 for different network structures. In the left part of Fig. 4, we present the betweenness centrality, closeness centrality, approximated Shapley value, and approximated

⁶“Karate-34” and “karate-empty-34” refer to a one-layer Zachary’s karate club network and to a two-layer network with Zachary’s karate club network in external layer and empty internal layer respectively, i.e. d_I does not exist for these two structures, in particular, it is equal to infinity. But in Fig. 3a, we replace infinity by number 99.

Myerson value for Nodes 0 and 33 on the simplified one-layer weighted network with weights calculated by formula (3). In the right part of Fig. 4, we present the group degree centrality, group closeness centrality, group betweenness centrality, and two different random walk centralities for the two-layer network with different internal structures. By comparing the centrality trend of Node 0 and Node 33 in the left and right parts of Fig. 4, respectively, we can observe that both have a similar trend, and this result demonstrates the validity of our approach of simplifying the two-layer network to a one-layer weighted network.

- Fig. 5 shows how KPIs vary with different network structures. Looking at Fig. 4, we may notice that some centralities trend of Node 33 are very similar to the trend in Fig. 3a. Fig. 3b also demonstrates the similar trend as in Fig. 5b.
- Fig. 5a shows that network structure has a great impact on winning rate.
- From Fig. 5b and 3b, we can notice that there exists a relationship between internal density D_I and consensus time T_{cons} . Networks with higher density, like “karate-complete-34”, take more time to reach consensus, while networks with less density, like “karate-empty-34”, reach consensus faster. This can be explained by the fact that networks with higher density have more connections which makes it more difficult for a single opinion to dominate quickly.

The main conclusions from the above results are: (i) there is a negative correlation between internal average shortest path d_I and both internal density D_I and consensus time T_{cons} , (ii) the approach of simplifying the two-layer network into a one-layer weighted network is valid.

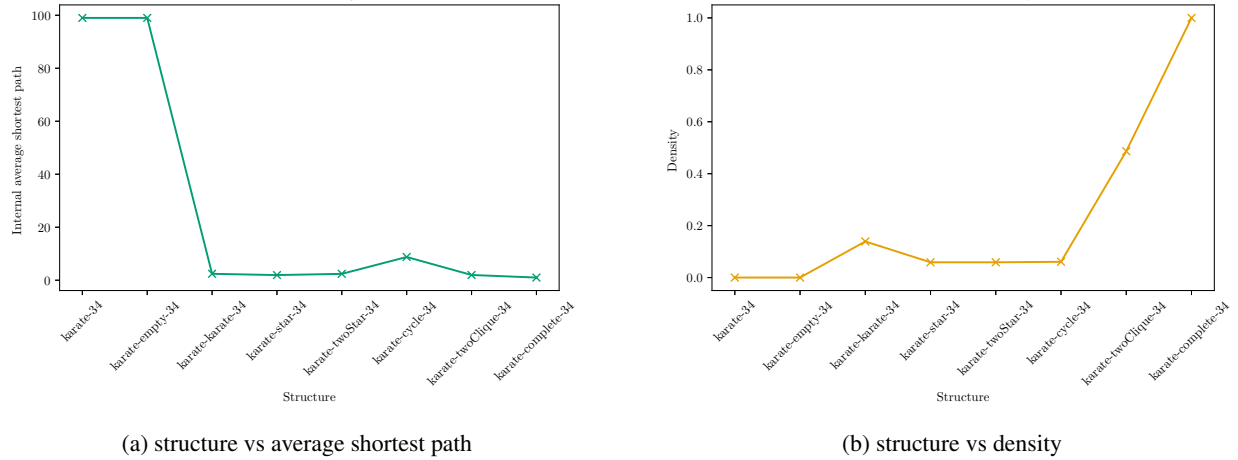


Figure 3: Internal average shortest path and density for different network structures

Our next step is to examine dependence of network structure and KPIs of opinion dynamics. To do this, we conducted correlation tests on the above observation results by SciPy [57, 58]. We calculated three coefficients for each pair of characteristics: Pearson [59], Kendall [60] Spearman [61] correlation coefficients. They are presented in Table 9, where *, **, *** represent a level of significance 0.05, 0.01, 0.001 of the correlation coefficient, respectively.⁷

We can make several conclusions from Table 9:

1. *High positive significant correlation:* (i) The internal density D_I exhibits a very strong highly significant positive correlation with consensus time across all correlation coefficients (Pearson, Kendall, and Spearman), they all are larger than 0.95. This indicates that when D_I increases, consensus time T_{cons} significantly increases; (ii) The internal average shortest path d_I is significantly positively correlated with most centrality measures which is confirmed by Kendall and Spearman correlation coefficients, they are significant.
2. *Negative significant correlation:* T_{cons} shows strong and significant negative correlation with network centrality measures like Betweenness and Closeness, especially with Closeness (with Pearson correlation coefficient equal to -0.928). So we can conclude that higher centrality scores are associated with shorter consensus time T_{cons} , which is expected.
3. *Variability in correlations:* Different metrics show varying levels of correlation strength across the Pearson, Kendall, and Spearman correlation coefficients. This variability indicates that the strength and significance of correlations can depend on the correlation method used, likely influenced by the underlying data distributions.

⁷We choose node 33 as the input for centrality. Actually, if we choose another node as an input, the conclusions are still valid.

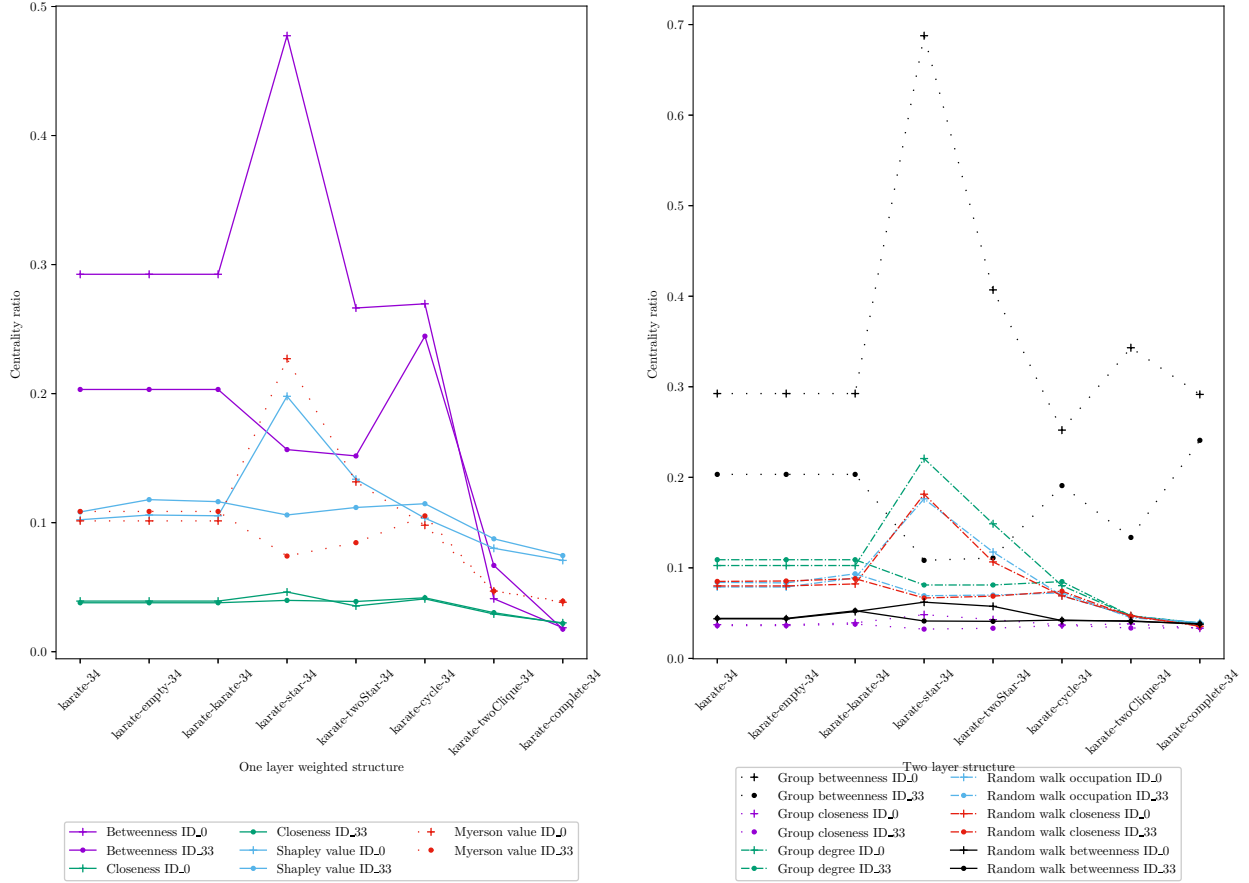
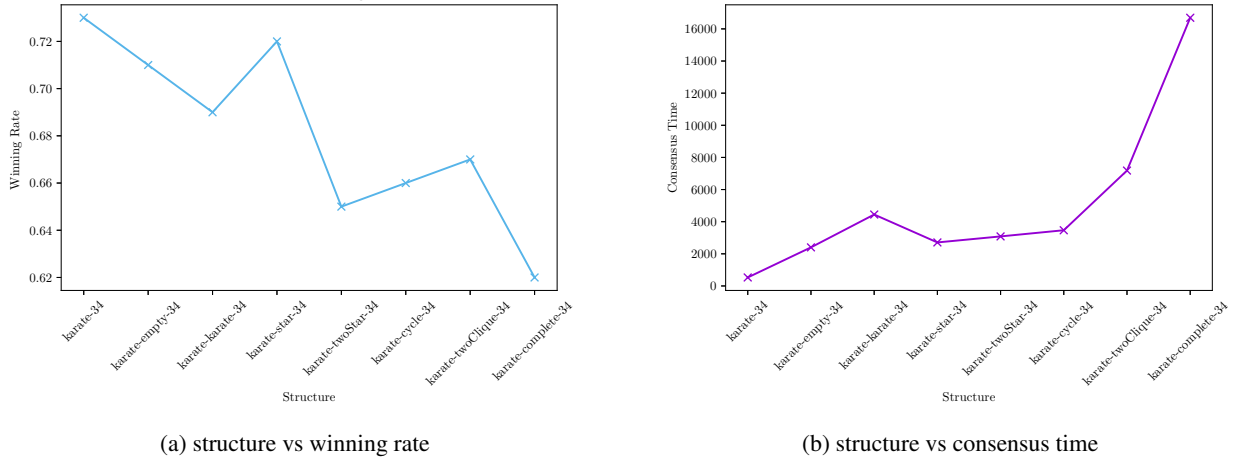


Figure 4: Different centralities for different structures



(a) structure vs winning rate

(b) structure vs consensus time

Figure 5: Winning rate and consensus time for different structures

To sum up, Table 9 highlights significant relationships between specific network properties and characteristics of opinion dynamics like consensus time. Centrality of authoritative nodes and network density play a crucial role for consensus time.

Table 9: Correlation coefficients

	Pearson	Kendall	Spearman
d_I vs Betweenness	0.414	0.654*	0.810*
d_I vs Closeness	0.231	0.192	0.270
d_I vs Shapley value	0.363	0.618*	0.766*
d_I vs Myerson value	0.548	0.808**	0.908**
d_I vs Group betweenness	0.366	0.185	0.157
d_I vs Group closeness	0.408	0.333	0.614
d_I vs Group degree	0.610	0.830**	0.933***
d_I vs Random walk occupation	0.475	0.691*	0.826*
d_I vs Random walk closeness	0.553	0.691*	0.826*
d_I vs Random walk betweenness	0.161	0.618*	0.778*
T_{cons} vs Betweenness	-0.841**	-0.491	-0.537
T_{cons} vs Closeness	-0.928***	-0.340	-0.464
T_{cons} vs Shapley value	-0.872**	-0.286	-0.452
T_{cons} vs Myerson value	-0.791*	-0.491	-0.659
T_{cons} vs Group betweenness	0.407	0.255	0.299
T_{cons} vs Group closeness	-0.291	0.109	0.036
T_{cons} vs Group degree	-0.807*	-0.593*	-0.771*
T_{cons} vs Random walk occupation	-0.785*	-0.429	-0.548
T_{cons} vs Random walk closeness	-0.834*	-0.357	-0.524
T_{cons} vs Random walk betweenness	-0.424	-0.500	-0.571
D_I vs T_{cons}	0.983***	0.964**	0.988***

5 Conclusions and future work

We proposed two fast and accurate algorithms to calculate centrality measures based on game-theoretic approach. Our algorithms can efficiently approximate the theoretical values of these measure for the networks, for which exact values are computationally difficult to find. Both of our algorithms can identify the most important nodes in the network, which is tested on different examples. The ideas of finding approximated centrality measures in the graphs implemented in our algorithms can be easily transferred to other fields, such as explainable artificial intelligence.

We examined the correlation of several characteristics of opinion dynamics (including BVM, CVM, and GCVM) realized on two-layer networks with characteristics of these networks. As a network in one layer we consider a Zachary’s karate club. We examined how internal network structure affects consensus time and winning rate, and if these key performance indicators correlate with network centrality measures.

We find the following developments of our work interesting: (i) improve the accuracy of the algorithms presented in the paper by improving sampling procedures and to test them on large networks, (ii) exploring the reasons of winning rate variation with the changes in network structure, (iii) obtain analytical expressions (in expectation sense) for approximated Shapley/Myerson values proposed in this paper.

References

- [1] LW McKeehan. A contribution to the theory of ferromagnetism. *Physical Review*, 26(2):274, 1925.
- [2] Katarzyna Sznajd-Weron and Jozef Sznajd. Opinion evolution in closed community. *International Journal of Modern Physics C*, 11(06):1157–1165, 2000.
- [3] Richard A Holley and Thomas M Liggett. Ergodic theorems for weakly interacting infinite systems and the voter model. *The Annals of Probability*, pages 643–663, 1975.
- [4] Michael T Gastner, Beáta Oborny, and Máté Gulyás. Consensus time in a voter model with concealed and publicly expressed opinions. *Journal of Statistical Mechanics: Theory and Experiment*, 2018(6):063401, 2018.
- [5] Michael T Gastner, Károly Takács, Máté Gulyás, Zsuzsanna Szvetelszky, and Beáta Oborny. The impact of hypocrisy on opinion formation: A dynamic model. *PloS one*, 14(6):e0218729, 2019.
- [6] Chi Zhao and Elena Parilina. Opinion dynamics in two-layer networks with hypocrisy. *Journal of the Operations Research Society of China*, 12(1):109–132, Mar 2024. ISSN 2194-6698. doi:10.1007/s40305-023-00503-2. URL <https://doi.org/10.1007/s40305-023-00503-2>.

- [7] Morris H DeGroot. Reaching a consensus. *Journal of the American Statistical Association*, 69(345):118–121, 1974.
- [8] Noah E Friedkin and Eugene C Johnsen. Social influence and opinions. *Journal of Mathematical Sociology*, 15(3-4):193–206, 1990.
- [9] Guillaume Deffuant, David Neau, Frederic Amblard, and Gérard Weisbuch. Mixing beliefs among interacting agents. *Advances in Complex Systems*, 3(01n04):87–98, 2000.
- [10] Rainer Hegselmann and Ulrich Krause. Opinion dynamics and bounded confidence models, analysis and simulation. *Journal of Artificial Societies and Social Simulation*, 5, 2002.
- [11] Sergey E Parsegov, Anton V Proskurnikov, Roberto Tempo, and Noah E Friedkin. Novel multidimensional models of opinion dynamics in social networks. *IEEE Transactions on Automatic Control*, 62(5):2270–2285, 2016.
- [12] Sadegh Bolouki, Roland P. Malhame, Milad Siami, and Nader Motee. Éminence grise coalitions: On the shaping of public opinion. *IEEE Transactions on Control of Network Systems*, 4(2):133 – 145, 2017. doi:10.1109/TCNS.2015.2482218.
- [13] Yulia Kareeva, Artem Sedakov, and Mengke Zhen. Influence in social networks with stubborn agents: From competition to bargaining. *Applied Mathematics and Computation*, 444:127790, 2023. ISSN 0096-3003. doi:<https://doi.org/10.1016/j.amc.2022.127790>. URL <https://www.sciencedirect.com/science/article/pii/S009630032200858X>.
- [14] Vladimir Mazalov and Elena Parilina. The euler-equation approach in average-oriented opinion dynamics. *Mathematics*, 8(3), 2020. ISSN 2227-7390. doi:10.3390/math8030355. URL <https://www.mdpi.com/2227-7390/8/3/355>.
- [15] M.A. Rogov and A.A. Sedakov. Coordinated influence on the opinions of social network members. *Automation and Remote Control*, 81:528–547, 2020.
- [16] D. A. Gubanov. Methods for analysis of information influence in active network structures. *Automation and Remote Control*, 83(5):743–754, 2022. doi:10.1134/S0005117922050071.
- [17] D.A. Gubanov and A.G. Chkhartishvili. Influence levels of users and meta-users of a social network. *Automation and Remote Control*, 79(3):545–553, 2018.
- [18] Carmela Bernardo, Claudio Altafini, Anton Proskurnikov, and Francesco Vasca. Bounded confidence opinion dynamics: A survey. *Automatica*, 159:111302, 2024. ISSN 0005-1098. doi:<https://doi.org/10.1016/j.automatica.2023.111302>. URL <https://www.sciencedirect.com/science/article/pii/S0005109823004661>.
- [19] Hossein Noorazar. Recent advances in opinion propagation dynamics: A 2020 survey. *The European Physical Journal Plus*, 135:1–20, 2020.
- [20] Quanbo Zha, Gang Kou, Hengjie Zhang, Haiming Liang, Xia Chen, Cong-Cong Li, and Yucheng Dong. Opinion dynamics in finance and business: a literature review and research opportunities. *Financial Innovation*, 6:1–22, 2020.
- [21] Ch. Zhao and E. M. Parilina. Analysis of consensus time and winning rate in two-layer networks with hypocrisy of different structures. *Vestnik of Saint Petersburg University. Applied Mathematics. Computer Science. Control Processes*, 20(2):170–192, 2024. doi:10.21638/11701/spbu10.2024.204.
- [22] Chi Zhao and Elena Parilina. Consensus time and winning rate based on simulations in two-layer networks with hypocrisy. In *2023 7th Scientific School Dynamics of Complex Networks and their Applications (DCNA)*, pages 68–71, 2023. doi:10.1109/DCNA59899.2023.10290478.
- [23] Vladimir Mazalov and Julia V Chirkova. *Networking games: network forming games and games on networks*. Academic Press, 2019.
- [24] Linton C Freeman. A set of measures of centrality based on betweenness. *Sociometry*, pages 35–41, 1977.
- [25] Alex Bavelas. Communication patterns in task-oriented groups. *The Journal of the Acoustical Society of America*, 22(6):725–730, 1950.
- [26] Linton C. Freeman. Centrality in social networks conceptual clarification. *Social Networks*, 1(3):215–239, 1978. ISSN 0378-8733. doi:[https://doi.org/10.1016/0378-8733\(78\)90021-7](https://doi.org/10.1016/0378-8733(78)90021-7). URL <https://www.sciencedirect.com/science/article/pii/0378873378900217>.
- [27] Gert Sabidussi. The centrality index of a graph. *Psychometrika*, 31(4):581–603, 1966.

- [28] James Powell and Matthew Hopkins. 9 - library networks—coauthorship, citation, and usage graphs. In James Powell and Matthew Hopkins, editors, *A Librarian's Guide to Graphs, Data and the Semantic Web*, Chandos Information Professional Series, pages 75–81. Chandos Publishing, 2015. ISBN 978-1-84334-753-8. doi:<https://doi.org/10.1016/B978-1-84334-753-8.00009-9>. URL <https://www.sciencedirect.com/science/article/pii/B9781843347538000099>.
- [29] Albert Solé-Ribalta, Manlio De Domenico, Sergio Gómez, and Alex Arenas. Random walk centrality in interconnected multilayer networks. *Physica D: Nonlinear Phenomena*, 323:73–79, 2016.
- [30] Mark EJ Newman. A measure of betweenness centrality based on random walks. *Social networks*, 27(1):39–54, 2005.
- [31] Mateusz K Tarkowski, Tomasz P Michalak, Talal Rahwan, and Michael Wooldridge. Game-theoretic network centrality: A review. *arXiv preprint arXiv:1801.00218*, 2017.
- [32] Lloyd S Shapley et al. A value for n-person games. 1953.
- [33] Roger B Myerson. Graphs and cooperation in games. *Mathematics of Operations Research*, 2(3):225–229, 1977.
- [34] N Rama Suri and Yadati Narahari. Determining the top-k nodes in social networks using the shapley value. In *Proceedings of the 7th International Joint Conference on Autonomous Agents and Multiagent Systems – Volume 3*, pages 1509–1512, 2008.
- [35] Vladimir V Mazalov, KE Avrachenkov, LI Trukhina, and Bulat T Tsynguev. Game-theoretic centrality measures for weighted graphs. *Fundamenta Informaticae*, 145(3):341–358, 2016.
- [36] Vladimir V Mazalov and VA Khitraya. A modified myerson value for determining the centrality of graph vertices. *Automation and Remote Control*, 82:145–159, 2021.
- [37] VA Khitraya and VV Mazalov. Game-theoretic centrality of directed graph vertices. *Automation and Remote Control*, 85(2), 2024.
- [38] Paolo Boldi and Sebastiano Vigna. Axioms for centrality. *Internet Mathematics*, 10(3-4):222–262, 2014.
- [39] Chi Zhao and Elena M. Parilina. Network structure properties and opinion dynamics in two-layer networks with hypocrisy. In Anton Ereemeev, Michael Khachay, Yury Kochetov, Vladimir Mazalov, and Panos Pardalos, editors, *Mathematical Optimization Theory and Operations Research*, pages 300–314, Cham, 2024. Springer Nature Switzerland. ISBN 978-3-031-62792-7.
- [40] Ginestra Bianconi. *Multilayer networks: structure and function*. Oxford University Press, 2018.
- [41] Wayne W Zachary. An information flow model for conflict and fission in small groups. *Journal of Anthropological Research*, 33(4):452–473, 1977.
- [42] Dense graph - wikipedia. https://en.wikipedia.org/wiki/Dense_graph. (Accessed on 02/20/2024).
- [43] Martin G Everett and Stephen P Borgatti. The centrality of groups and classes. *The Journal of Mathematical Sociology*, 23(3):181–201, 1999.
- [44] Martin G Everett and Stephen P Borgatti. Extending centrality. *Models and Methods in Social Network Analysis*, 35(1):57–76, 2005.
- [45] Junzhou Zhao, John CS Lui, Don Towsley, and Xiaohong Guan. Measuring and maximizing group closeness centrality over disk-resident graphs. In *Proceedings of the 23rd International Conference on World Wide Web*, pages 689–694, 2014.
- [46] Fan RK Chung. *Spectral graph theory*, volume 92. American Mathematical Soc., 1997.
- [47] Mark Newman. *Networks: An Introduction*. Oxford University Press, 03 2010. ISBN 9780199206650. doi:10.1093/acprof:oso/9780199206650.001.0001. URL <https://doi.org/10.1093/acprof:oso/9780199206650.001.0001>.
- [48] Linton C Freeman, Stephen P Borgatti, and Douglas R White. Centrality in valued graphs: A measure of betweenness based on network flow. *Social Networks*, 13(2):141–154, 1991.
- [49] Karen Stephenson and Marvin Zelen. Rethinking centrality: Methods and examples. *Social networks*, 11(1):1–37, 1989.
- [50] L. Lovász. Random walks on graphs: A survey. *Combinatorics, Paul Erdos is Eighty*, 2(1):1–46, 1993. URL http://scholar.google.de/scholar.bib?q=info:llcRghStI1oJ:scholar.google.com/&output=citation&hl=de&as_sdt=0,5&ct=citation&cd=3.
- [51] Zhongzhi Zhang, Alafate Julaiti, Baoyu Hou, Hongjuan Zhang, and Guanrong Chen. Mean first-passage time for random walks on undirected networks. *The European Physical Journal B*, 84:691–697, 2011.

- [52] John G Kemeny, J Laurie Snell, et al. *Finite markov chains*, volume 26. van Nostrand Princeton, NJ, 1969.
- [53] Georg Pólya. Eine wahrscheinlichkeitsaufgabe in der kundenwerbung. *Zamm-zeitschrift Fur Angewandte Mathematik Und Mechanik*, 10:96–97, 1930. URL <https://api.semanticscholar.org/CorpusID:123056679>.
- [54] Matthew O Jackson et al. *Social and economic networks*, volume 3. Princeton University Press: Princeton, 2008.
- [55] Vladimir V Mazalov and Lyudmila I Trukhina. Generating functions and the myerson vector in communication networks. *Discrete Mathematics and Applications*, 24(5):295–303, 2014.
- [56] Stanley Milgram. The small world problem. *Psychology Today*, 2(1):60–67, 1967.
- [57] `scipy.stats.pearsonr` — `scipy v1.12.0 manual`. <https://docs.scipy.org/doc/scipy/reference/generated/scipy.stats.pearsonr.html>. (Accessed on 02/11/2024).
- [58] Pauli Virtanen, Ralf Gommers, Travis E. Oliphant, Matt Haberland, Tyler Reddy, David Cournapeau, Evgeni Burovski, Pearu Peterson, Warren Weckesser, Jonathan Bright, Stéfan J. van der Walt, Matthew Brett, Joshua Wilson, K. Jarrod Millman, Nikolay Mayorov, Andrew R. J. Nelson, Eric Jones, Robert Kern, Eric Larson, C J Carey, İlhan Polat, Yu Feng, Eric W. Moore, Jake VanderPlas, Denis Laxalde, Josef Perktold, Robert Cimrman, Ian Henriksen, E. A. Quintero, Charles R. Harris, Anne M. Archibald, Antônio H. Ribeiro, Fabian Pedregosa, Paul van Mulbregt, and SciPy 1.0 Contributors. SciPy 1.0: Fundamental Algorithms for Scientific Computing in Python. *Nature Methods*, 17:261–272, 2020. doi:10.1038/s41592-019-0686-2.
- [59] STUDENT. PROBABLE ERROR OF A CORRELATION COEFFICIENT. *Biometrika*, 6(2-3):302–310, 09 1908. ISSN 0006-3444. doi:10.1093/biomet/6.2-3.302. URL <https://doi.org/10.1093/biomet/6.2-3.302>.
- [60] Maurice G Kendall. The treatment of ties in ranking problems. *Biometrika*, 33(3):239–251, 1945.
- [61] Charles Spearman. The proof and measurement of association between two things. *The American Journal of Psychology*, 100(3/4):441–471, 1987.